A computational study of possible mechanisms of singlet oxygen generation in miniSOG photoactive protein

Goran Giudetti[a], Anastasia R. Blinova[b], Bella L. Grigorenko[b], and Anna I. Krylov[a]

[a] Department of Chemistry, University of Southern California, Los Angeles, CA 90089, U.S.A.

[b] Department of Chemistry, Lomonosov Moscow State University, Moscow, 119991, Russia

We report high-level electronic structure calculations of electronic states in the miniSOG (for mini Singlet Oxygen Generator) photoactive protein designed to produce singlet oxygen upon light exposure. We consider a model system with a riboflavin (RF) chromophore. To better understand the photosensitization process, we compute relevant electronic states of the combined oxygen-chromophore system and their couplings. The calculations suggest that singlet oxygen can be produced both by inter-system crossing, via a triplet state of the RF(T_1)×O_2($^3\Sigma_g^-$) character as well as by triplet excitation energy transfer via a singlet state of the same character. Importantly, the former channel produces $O_2(^1\Sigma_g^+)$, an excited state of singlet oxygen, which is known to convert with unit efficiency into $O_2(^1\Delta_g)$ The calculations also provide evidence for the production of the triplet state of the chromophore via internal conversion facilitated by oxygen. Our results provide concrete support to previously hypothesized scenarios.

I. INTRODUCTION

Genetically encodable photoactive proteins are used in a variety of applications[1,2]. Of particular interest are photoactive systems that can generate reactive oxygen species (ROS) upon exposure to light. The interest in such systems stems from their uses in electronic microscopy[3], photodynamic therapy[4], and chromophore-assisted laser cell inactivation[5]. One such protein is miniSOG (for mini Singlet Oxygen Generator)—a small (106 amino acid residues) flavin-containing protein capable of generating ROS when stimulated by blue light[6]. miniSOG is the first flavin-binding protein developed specifically as a genetically encodable light-induced source of singlet oxygen.

The chromophore in miniSOG is flavin mononucleotide (FMN), however, variants with a

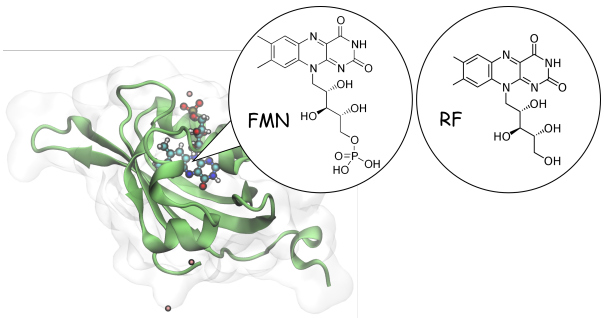

FIG. 1: miniSOG protein. Flavin mononucleotide (FMN) and riboflavin (RB) cofactors are shown in the inserts.

riboflavin (RF) cofactor have also been investigated[7,8]. Fig. 1 shows the miniSOG structure as well as structures of the FMN and RF chromophores.

Interestingly, the quantum yield of singlet oxygen production in miniSOG is much smaller than that in free FMN—i.e., 0.03 versus 0.51 (see, for example, Ref. 7), which is attributed to the effective quenching of the FMNs triplet state by the protein via electron transfer[7,9,10]. This undesirable quenching by the protein was also deemed responsible for producing other types of ROS, such as peroxide[9], which is undesirable for applications. Several studies reported modifications of miniSOG aiming to increase the quantum yield of singlet oxygen production[9,11]. For example, by mutating one residue forming a hydrogen bond with FMN, the quantum yield of $O_2(^1\Delta_g)$ was increased up to ~ 0.2 in SOPP (singlet oxygen producing protein)[9,11].

It was also discovered that prolonged intense irradiation of miniSOG leads to an increase of singlet oxygen production[12]. The mechanism for this photoactivation involves photodegradation of FMN to lumichrome (LC), which increases chromophore's accessibility to oxygen[7] thus making oxygen quenching more effective than protein quenching of the triplet chromophore. This mechanistic interpretation of the structural data[7] is consistent with observations that the yield of singlet oxygen increases in both miniSOG and SOPP at elevated temperatures[10] due to protein's breathing motions favorable for oxygen diffusion.

The photodegradation phenomenon has been investigated in dozens of studies, which considered both free flavins[13–24] and flavin-containing proteins[25,26], however, the exact details of the mechanism have not yet been fully elucidated. The mechanism of photosensitization in miniSOG is also not fully understood. Detailed molecular-level understanding of these processes is essential for the successful rational design of further miniSOG and SOPP variants

aiming to improve the quantum yield of singlet oxygen production and the spectral properties of the protein.

Questions about the mechanism involve identification of electronic states involved in photosensitization and in photoconversion[27–30]. This requires calculations of singlet and triplet states as well as relevant electronic couplings. In addition, characterization of the effect of the protein environment on these quantities is important, as it is known that they strongly depend on the polarity of the environment[31–33].

Many computational studies investigated SOCs in flavin proteins and flavin-like chromophores. For example, SOC calculations have been carried out to elucidate the reaction between FMN and neighboring cysteine in LOV domains[34], to estimate the influence of the protein environment on the excited states of flavin[35], to describe the reverse cycle FADH2→FAD, connected with the reduction of O_2 to H_2O_2 in glucose oxidase[36], to design fluorinated flavin derivatives with desired spectral properties[37], and so on.

The production of singlet oxygen[38] by photosensitization, a transfer of electronic excitation from an electronically excited donor to a ground-state acceptor, occurs in many systems. This process is responsible for the ability of oxygen to effectively quench both fluorescence (i.e., singlet excited states) and phosphorescence (i.e., triplet excited states). Unlike Förster energy transfer[39], which involves transfer of dipole-allowed excitations and can happen between distant moieties, the transfer of spin-forbidden electronic excitations (triplet excitons via Dexter energy transfer) can only occur when the donor and acceptor are in close proximity[40]. Hence, the accessibility of the chromophores to dissolved oxygen is the key factor determining the efficiency of singlet oxygen generation.

The nature of electronic couplings responsible for singlet oxygen production and quenching of singlet and triplet excited states by oxygen has been extensively debated[38,41–43]. Despite the limited computational power, earlier theoretical works have developed clear explanations of this process as well as related phenomena (e.g., ignition of slow fluorescence, singlet–triplet annihilation, etc)[42–45], which we can now confirm by high-level calculations. The two main scenarios of singlet oxygen production include intersystem crossing (ISC), facilitated by spin–orbit couplings (SOC), and internal conversion (IC), facilitated by nonadiabatic couplings[42–45]. We note that the latter process is promoted by configuration interactions with charge-transfer configurations[44] and is similar to singlet fission[46,47], a process of generating two triplet excitons from a single singlet exciton.

In this contribution, we report high-level electronic structure calculations using QM/MM approach[48,49]. We consider protein-bound flavin chromophore (RF) with and without nearby oxygen molecule. Our calculations provide quantitative support to earlier mechanistic proposals[42–44] put forward when computational power was not sufficient to carry out accurate *ab initio* calculations on realistic systems. Our results provide complimentary details to a large body of research on singlet oxygen generation by flavin-based systems.

II. COMPUTATIONAL DETAILS

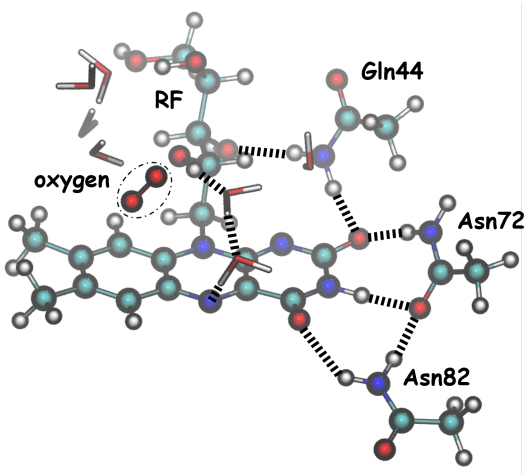

FIG. 2: QM cluster (model system A) used for QM/MM optimization and excited-state calculations: RF, O_2, sidechains of Gln77, Asn72, Asn82, and seven water molecules.

Our model structure was prepared in earlier work[50], where it was constructed using crystal structure of miniSOG with the RF cofactor (PDB ID 7QF4)[8]. Hydrogen atoms were added assuming the conventional protonation states of the polar residues at neutral pH: Arg and Lys were charged positively, Glu and Asp were charged negatively, and His85 was neutral. Following notations from Ref. 50, we refer to this model miniSOG[RF]. The initial structure was solvated and neutralized following the standard protocols, and ten dioxygen molecules were added to it at random places. The structure was then equilibrated using molecular dynamics (MD) with CHARMM36 forcefield topology and parameters[51], TIP3P water, and RF parameters in the oxidized form of flavin from Ref. 52; for details, see Ref. 50. Selected snapshots from equilibrium trajectories were optimized using QM/MM with the PBE0 functional[53] and the 6-31G* basis set, and using the AMBER99 forcefield parameters[54]

for the MM part. Our model structure corresponds to one of the snapshots with oxygen molecule in the close vicinity of the chromophore.

The QM system included RF, O_2, sidechains of Gln77, Asn72, and Asn82, and seven water molecules. This structure—called model A—was also used to compute electronic states and relevant couplings. The structure is shown in Fig. 2.

The excited-state calculations were done using several structures derived from model A: (i) model A, (ii) model A without oxygen molecule (model B), and (iii) model B with oxygen molecule placed far away from the chromophore (∼6-8 Å).

The excited states were computed using several approaches: TD-DFT (time-dependent density functional theory), RAS-CI (restricted active space configuration interaction)[55], and extended multiconfigurational quasi-degenerate perturbation theory of the second order (XMCQDPT2)[56]. The XMCQDPT2 calculations were based on state-averaged CASSCF(10/8)/cc-pVDZ wavefunctions (14 states were used in the averaging). Active-space orbitals are shown in the SI. Because in XMCQDPT2 singlets and triplets are computed separately, the relative total energies of different multiplicity manifolds are not accurate. To correct this mismatch, we shift the singlet manifold of the combined RF-O_2 system so that the excitation energy of the lowest state in the singlet manifold, which corresponds to $RF(S_0)\times O_2(^1\Delta_g)$ state, equals experimental[57] excitation energy of the $O_2(^3\Sigma_g^-)\rightarrow O_2(^1\Delta_g)$ transition (0.97 eV).

We carried out SOC calculations using RASCI and TD-DFT. TD-DFT calculations are suitable for computing singlet and triplet excited states of closed-shell molecules, such as RF and FMN. However, electronic degeneracies in oxygen impart open-shell character[58] to the wave-functions of relevant states. Such states can be tackled either by multi-reference methods, such as CASSCF, or by spin-flip approaches[59,60]. As we explain below, the RF-O_2 system can be tackled by a double spin-flip approach, in the same fashion as was done before in the context singlet fission[61–63]. The RAS-2SF calculations have employed quintet reference corresponding to the high-spin $RF(T_1) \times O_2(^3\Sigma_g^-)$ restricted open-shell Hartree–Fock determinant.

The SOCs were computed as matrix elements of the spin–orbit part of the Breit–Pauli Hamiltonian. The two-electron contributions were computed using mean-field approach[64–67].

TD-DFT and RAS-CI calculations were carried out using the Q-Chem electronic structure package[68,69]. XMCQDPT2 calculations were carried out by Firefly[70].

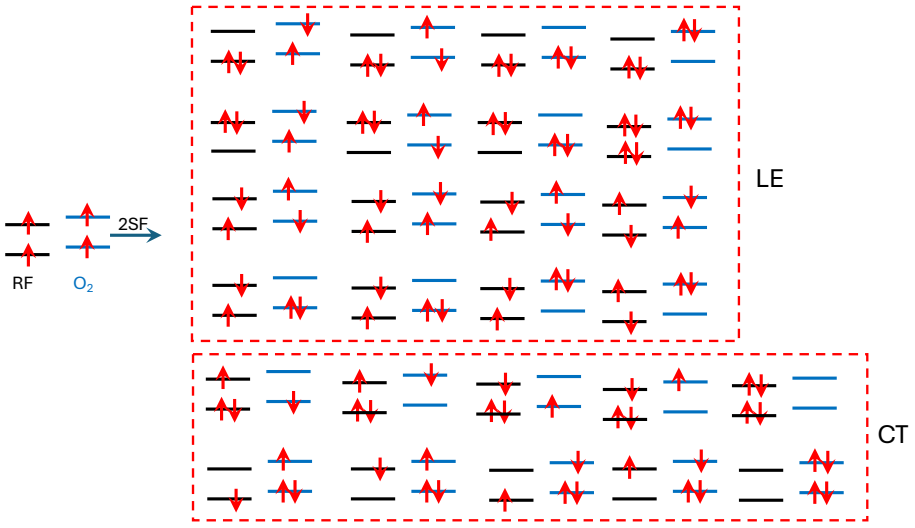

FIG. 3: RAS-2SF reference and target determinants. Singly occupied orbitals are flavin's π and π^* and oxygen's π_x^* and π_y^* LE and CT denote local excitations and charge-transfer configurations, respectively.

III. RESULTS AND DISCUSSION

We begin by reviewing the basic energetics of the RF chromophore and molecular oxygen. Molecular oxygen's ground state is $^3\Sigma_g^-$. The next two states are singlets: doubly degenerate $^1\Delta_g$ and $^1\Sigma_g^+$ states located at 0.97 eV and 1.63 eV, respectively[38,57]. The electronic configurations of these four states can be described by distributing two electrons in two degenerate π^* orbitals—they are shown in Fig. 4. There are four determinants—two of an open-shell type (in which the two π^* orbitals are singly occupied) and two of a closed-shell type (in which one of the orbitals is doubly occupied and the second is empty). According to the El-Sayed rules,[71], one can anticipate small (or zero) SOCs between the determinants of the same type and large SOCs between the closed-shell and open-shell determinants—since these are related by a transition between π_x^* and π_y^* and thus involve an orbital flip. To understand the SOCs between these states, recall that each state is described by two determinants, so the combined effect depends on the relative signs (a similar situation was described in Ref. 72). By analyzing the configurations in Fig. 4, one can see that the SOC between the $^3\Sigma_g^-$ and $^1\Delta_g$ is expected to be small (contributions from the two determinants cancel out) whereas the SOC between the $^3\Sigma_g^-$ and $^1\Sigma_g^+$ can be large (contributions from open-shell-closed shell transitions add up). The calculation of SOCs confirms this—at the RAS-SF/6-311G(d,p) level of theory, the respective SOCs are 0.00 and 173.36 cm^{-1}.

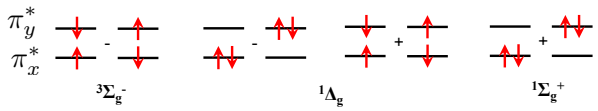

FIG. 4: Electronic configurations of the $^3\Sigma_g^-$, $^1\Delta_g$, and $^1\Sigma_g^+$ states of molecular oxygen.

TABLE I: Excitation energies (eV) for model system B (no oxygen). Oscillator strengths for the transitions from RF(S_0) are given in parenthesis.

State	ωB97MV/aug-cc-pVTZ	XMCQDPT2/cc-pVDZ[a]
S_1	3.26 (0.33)	2.99 (0.42)
S_2	3.84 (0.02)	3.71 (0.20)
T_1	2.16	2.62
T_2	2.82	3.05
T_3	3.41	3.34

[a]XMCQDPT2 is based on SA14-CASSCF(10/8) wavefunctions. The XMCQDPT2 calculations were carried out for a model structure with oxygen molecule far away from RF (see text for details).

Table I lists energies of the RF chromophore in the model miniSOG[RF] system; additional results are given in the SI. The computed energetics is similar to other flavin-based systems[37]: at the XMCQDPT2 level, the lowest triplet state is ∼0.3 eV below S_1, and the second triplet is slightly above S_1. TD-DFT slightly overestimates excitation energy of the singlet and underestimates energies of the triplets relative to XMCQDPT2, however, the overall picture is similar. Fig. 5 shows NTOs for the $S_0 \rightarrow T_1$ and $S_0 \rightarrow S_1$ transitions in RF (model system B). The shape of NTOs is similar, consistent with $\pi \rightarrow \pi^*$ character of the transitions. Because the two states have similar orbital character, the S_1-T_1 SOC is expected to be small by virtue of El-Sayed's rules[71], as confirmed by the calculations.

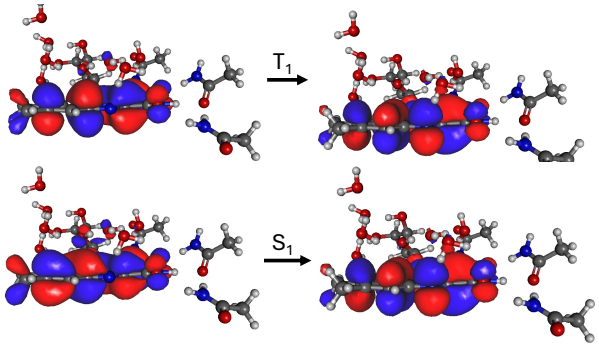

FIG. 5: NTOs for the two lowest transitions in RF cofactor in miniSOG[RF].

Such small values of $S_0 \rightarrow T_1$ SOCs in flavin-based systems have been reported by previous

studies[34,37]. They might appear puzzling in view of a high quantum efficiency of triplet-state yields[10,73]—as high as 0.4-0.5. Such efficient ISC in flavins is facilitated by spin-vibronic interactions, which entail contributions from higher triplet states[37,74,75]. As we illustrate below, the production of triplet RF can be also enhanced by molecular oxygen via IC, as was observed experimentally[38,41–43].

To investigate possible pathways of the singlet oxygen production, we consider a model system that comprises the RF chromophore and a nearby oxygen molecule, embedded in the protein (model system A, see Computational Details). The low-lying electronic states of the combined RF-O_2 system can be described as products of $\Psi(\mathrm{RF}) \times \Psi(\mathrm{O_2})$, and their energies can be estimated as a sum of the respective energies of the two moieties. We note that electronic configurations of these composite states are derived by distributing four electrons in the four orbitals—π and π^* orbitals of RF and two π^* orbitals of oxygen, a situation suitable for double spin-flip approach using a high-spin quintet reference (see Fig. 3)[60,76].

Fig. 6 shows energy diagram for the singlet and triplet manifolds obtained by combining energies of the isolated O_2 and RF (taken from model system B) using experimental energies for O_2 and our best estimates for the RF chromophore. Table II shows the results of XMCQDPT2 calculations for system A. The RAS-2SF results are given in the SI. The RAS-2SF energies are less accurate then XMCQDPT2 due to an insufficient description of dynamic correlation. Inclusion of *hp* (hole-particle) excitations improves the results significantly, althougth the changes in the wavefunctions are minimal.

We note that a similar energy diagram was invoked by Tsubomura and Mulliken in 1960[42] and by Minaev[44]. Overall, the presence of O_2 has a negligible effect on the states' energies, as expected for this weakly interacting complex, so that the energy diagram in Fig. 6 provides a good description of energy levels.

As one can see, upon excitation to the S_1 state of RF, several pathways for electronic relaxation are energetically possible in the triplet and singlet manifolds. The accessible states are: $\mathrm{RF}(T_1)\times\mathrm{O_2}(^3\Sigma_g^-)$, $\mathrm{RF}(S_0)\times\mathrm{O_2}(^1\Sigma_g^+)$, and $\mathrm{RF}(S_0)\times\mathrm{O_2}(^1\Delta_g)$.

To further analyze these pathways, we consider relevant electronic couplings—SOCs between states different multiplicity and NACs between the states of the same multiplicity. As a proxy for NAC, we consider the norm of one-particle transition density matrix, $||\gamma||$, between the two states[61,77] (large $||\gamma||$ signifies considerable one-electron character of the transition, which can develop due to the admixture of charge-transfer configurations). Fig. 7 shows

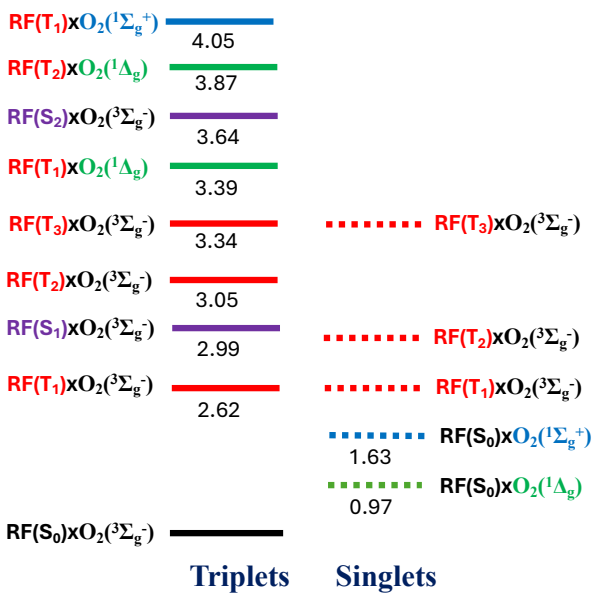

FIG. 6: Energy diagram of the low-lying manifold of singlet and triplet states derived from RF's S_0, S_1, S_2, T_1, and T_2 and oxygen's $^3\Sigma_g^-$, $^1\Delta_g$, and $^1\Sigma_g^+$. Excitation energies in electron-volt relative to the ground state, RF(S_0) × $O_2(^3\Sigma_g^-)$.

TABLE II: Excitation energies (eV) for model system A; XMCQDPT2/cc-pVDZ. Oscillator strength for the transitions from RF(S_0) are given in parenthesis.

State	Multiplicty	E_{ex}, eV
RF(S_0)×$O_2(^3\Sigma_g^-)$	triplet	0.0
RF(S_0)×$O_2(^1\Delta_g)$	singlet	0.97
RF(S_0)×$O_2(^1\Delta_g)$	singlet	0.97
RF(S_0)×$O_2(^1\Sigma_g^+)$	singlet	1.64
RF(T_1)×$O_2(^3\Sigma_g^-)$	triplet	2.62
RF(S_1)×$O_2(^3\Sigma_g^-)$	triplet	2.99 (0.422)
RF(T_2)×$O_2(^3\Sigma_g^-)$	triplet	3.04
RF(S_2)×$O_2(^3\Sigma_g^-)$	singlet	3.70 (0.204)
RF(T_1)×$O_2(^1\Delta_g)$	triplet	3.74
RF(T_1)×$O_2(^1\Delta_g)$	triplet	3.74
RF(S_1)×$O_2(^1\Delta_g)$	singlet	4.02
RF(S_1)×$O_2(^1\Delta_g)$	singlet	4.02

XMCQDPT2 is based on SA14-CASSCF(10/8) wavefunctions (see text for details).

the computed couplings. First, we consider the initially excited state, RF(S_1)×$O_2(^3\Sigma_g^-)$ (its multiplicity is triplet because of oxygen). The values of SOC that couples this state to the singlet state RF(T_1)×$O_2(^3\Sigma_g^-)$ is small (as expected from the SOC value for the T_1-S_1 coupling in RF. The value of SOC with RF(S_0)×$O_2(^1\Delta_g)$ state is also small (0.19 cm^{-1}). Thus, a single-step electronic transition producing $O_2(^1\Delta_g)$ is possible, but does not appear

to be very effective. However, the initially excited state shows a substancial NAC with a *triplet* RF(T_1)×O_2($^3\Sigma_g^-$), suggesting that this non-adiabatic transition can be fast and effective. This means that the production of triplet RF can proceed both via ISC and via IC, when oxygen is present. Such an oxygen-assisted pathway for the triplet production has been put forward by Tsubomura and Mulliken in 1960[42] to explain enhanced ISC—an increased yield of triplet states in the presence of oxygen—first discussed by Kasha in 1950[78]. This enhancement was also documented by Minaev and co-workers, who provided a theoretical support using semi-empirical calculations on a model system[44]. Tsubomura and Mulliken also posited that sufficiently large coupling between these states can develop via configuration interaction mixing of charge-transfer configurations[42], which was later illustrated by Minaev's calculations[44]. We note that the admixture of charge-transfer (or charge-resonance) configurations is also responsible for couplings facilitating singlet fission[61] and triplet–triplet annihilation[79,80].

We now consider possible transitions of the RF(T_1)×O_2($^3\Sigma_g^-$). The singlet state of this character can be produced by either non-adiabatic transition described above or by a collision of oxygen molecule with the RF(T_1) state formed by ISC. According Fig. 7, the singlet state of this character features no significant couplings with lower states and is, therefore, not very effective for singlet oxygen generation. The reason why this state does not couple with the lower states in the singlet manifold is because the respective transitions would involve changes of states of two electrons, which means that the only coupling terms can come from the exchange interaction, as in the Dexter energy transfer[81]—such transitions are possible, but not very effective. In contrast, the triplet state of this character shows large SOC with the RF(S_0)×O_2($^1\Sigma_g^+$) state. Hence, ISC from this state can lead to the production of O_2($^1\Sigma_g^+$). This other singlet oxygen has been observed experimentally[73]. It relaxes to O_2($^1\Delta_g$) with unit efficiency[73]. The computed value of the NAC for the RF(S_0)×O_2($^1\Sigma_g^+$) → RF(S_0)×O_2($^1\Delta_g$) transition is large, consistent with the experimental observations[73]. This large value suggests very fast internal conversion, which can outcompete ISC to the ground state of the system, RF(S_0)×O_2($^3\Sigma_g^-$). Once the RF(S_0)×O_2($^1\Delta_g$) state is formed, the only energetically allowed pathway leading to the ground state and regeneration of triplet oxygen is suppressed by virtue of the zero SOC. Hence, the resulting singlet oxygen can diffuse away without being quenched by the chromophore.

Our results are consistent with previous mechanistic discussions of the singlet oxygen

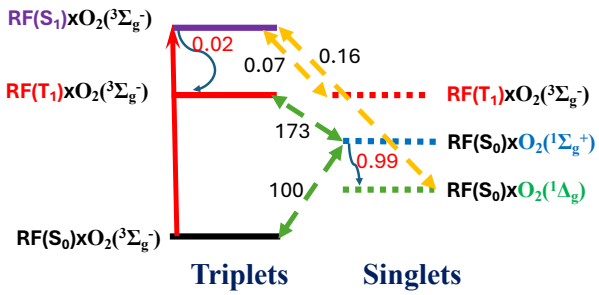

FIG. 7: Couplings between the relevant states. SOC values (in cm^{-1}) are shown in black and $||\gamma||$ values (dimensionless) are shown in red. For the degenerate $^1\Delta_g$ states, the combined SOC is shown.

production[38,44,73]. The value of our contribution is that by providing concrete values of the electronic couplings it lands *ab initio* support to previously hypothesized scenarios. We note that the pathway of singlet oxygen production via a *triplet* state of the oxygen-RF collision complex means that the kinetic models used to describe singlet oxygen production in flavin-based systems (such as one in Ref. 10) need to be adjusted to account for different spin statistics.

IV. CONCLUSION

We report high-level quantum chemistry calculations of a model system representing miniSOG photoactive protein with the RF chromophore. Our calculations of relevant electronic states and couplings between them clarify the mechanism of singlet oxygen generation in this system. In particular, our results indicate that the doorway state for singlet oxygen generation is the triplet $\mathrm{RF}(\mathrm{S}_1)\times\mathrm{O}_2(^3\Sigma_g^-)$ state of the RF-O_2 complex whereas the corresponding singlet state is less effective owing to small couplings. The triplet $\mathrm{RF}(\mathrm{S}_1)\times\mathrm{O}_2(^3\Sigma_g^-)$ state can be produced either by IC of the initially excited S_1 state of RF bound to oxygen or by the T_1 state of RF (produced via ISC) forming a collision complex with O_2. This state can decay via ISC into $\mathrm{RF}(\mathrm{S}_0)\times\mathrm{O}_2(^1\Sigma_g^+)$. The $\mathrm{O}_2(^1\Sigma_g^+)$ effectively converts to $\mathrm{O}_2(^1\Delta_g)$.

Our results provide robust theoretical support to previously hypothesized scenarios. We hope that a better understanding the function of miniSOG will aid further development of effective genetically encoded photoactive proteins. Future work will focus on quantitative calculations of rates of the relevant processes and mechanisms of photodegradation and production of other types of ROS—such as peroxide—in these systems.

Acknowledgment

We acknowledge support from the National Science Foundation (grant No. CHE-2154482 to A.I.K.) and resources of USC Advanced Research Computing (CARC) facilities. The Moscow team was supported by the Russian Science Foundation (project 22-13-00012). The research in Moscow was carried out using the equipment of the shared research facilities of HPC computing resources at the Lomonosov Moscow State University and supercomputer resources of the Joint Supercomputer Center of the Russian Academy of Sciences.

Conflicts of interest

The authors declare the following competing financial interest(s): A.I.K. is the president and a part-owner of Q-Chem, Inc.

Data availability

The data that support the findings of this study are available within the article and the associated SI.

---

[1] D.M. Chudakov, M.V. Matz, S. Lukyanov, and K.A. Lukyanov, Fluorescent proteins and their applications in imaging living cells and tissues, Physiol. Rev. **90**, 1103 (2010).

[2] A. Acharya, A. M. Bogdanov, K. B. Bravaya, B. L. Grigorenko, A. V. Nemukhin, K. A. Lukyanov, and A. I. Krylov, Photoinduced chemistry in fluorescent proteins: Curse or blessing?, Chem. Rev. **117**, 758 (2017).

[3] C. Smith, Two microscopes are better than one, Nature **492**, 293 (2012).

[4] D. L. Sai, J. Lee, D. L. Nguyen, and Y.-P. Kim, Tailoring photosensitive ROS for advanced photodynamic therapy, Exp. & Mol. Med. **53**, 495 (2021).

[5] M. A. McLean, Z. Rajfur, Z. Chen, D. Humphrey, B. Yang, S. G. Sligar, and Ken Jacobson, Mechanism of chromophore assisted laser inactivation employing fluorescent proteins, Anal. Chem. **81**, 1755–1761 (2001).

[6] X. Shu, V. Lev-Ram, T. J. Deerinck, Y. Qi, E. B. Ramko, M. W. Davidson, Y. Jin, M. H. Ellisman, and R. Y. Tsien, A genetically encoded tag for correlated light and electron microscopy of intact cells, tissues, and organisms, PLos Biol. **9**, e1001041 (2011).

[7] J. Torra, C. Lafaye, L. Signor, S. Aumonier, C. Flors, X. Shu, S. Nonell, G. Gotthard, and A. Royant, Tailing miniSOG: structural bases of the complex photophysics of a flavin-binding singlet oxygen photosensitizing protein, Sci. Rep. **9**, 2428 (2019).

[8] C. Lafaye, S. Aumonier, J. Torra, L. Signor, D. von Stetten, M. Noirclerc-Savoye, X. Shu, R. Ruiz-González, G. Gotthard, A. Royant, and Nonell, Riboflavin-binding proteins for singlet oxygen production, Photochem. Photobiol. Sci. **21**, 1545 (2022).

[9] M. Westberg, L. Holmegaard, F. M. Pimenta, M. Etzerodt, and P. R. Ogilby, Rational design of an efficient, genetically encodable, protein-encased singlet oxygen photosensitizer, J. Am. Chem. Soc. (2015).

[10] M. Westberg, M. Bregnhøj, M. Etzerodt, and P. R. Ogilby, Temperature sensitive singlet oxygen photosensitization by LOV-derived fluorescent flavoproteins, J. Phys. Chem. B **121**, 2561 (2017).

[11] M. Westberg, M. Bregnhøj, M. Etzerodt, and P. R. Ogilby, No photon wasted: An efficient and selective singlet oxygen photosensitizing protein, J. Phys. Chem. B **121**, 9366 (2017).

[12] R. Ruiz-González, A. L. Cortajarena, S. H. Mejias, M. Agut, S. Nonell, and C. Flors, Singlet oxygen generation by the genetically encoded tag miniSOG, **135**, 9564 (2013).

[13] W. Holzer, J. Shirdel, P. Zirak, A. Penzkofer, P. Hegemann, R. Deutzmann, and E. Hochmuth, Photo-induced degradation of some flavins in aqueous solution, Chem. Phys. **308**, 69 (2005).

[14] G. Strauss and W. J. Nickerson, Photochemical cleavage of water by riboflavin. II. Role of activators, J. Am. Chem. Soc. **83**, 3187 (1961).

[15] P. F. Heelis, The photophysical and photochemical properties of flavins (isoalloxazines), Chem. Soc. Rev. **11**, 15 (1982).

[16] M. Insińska-Rak, A. Golczak, and M. Sikorski, Photochemistry of riboflavin derivatives in methanolic solutions, J. Phys. Chem. A **116**, 1199 (2012).

[17] W. M. Moore, J. T. Spence, F. A. Raymond, and S. D. Colson, Photochemistry of riboflavin. I. The hydrogen transfer process in the anaerobic photobleaching of flavins, J. Am. Chem. Soc. **85**, 3367 (1963).

[18] M. Halwer, The photochemistry of riboflavin and related compounds, J. Am. Chem. Soc. **73**,

4870 (1951).

[19] M. Insińska-Rak, E. Sikorska, J. L. Bourdelande, I. V. Khmelinskii, W. Prukała, K. Dobek, J. Karolczak, I. F. Machado, L. F. V. Ferreira, E. Dulewicz, A. Komasa, D. R. Worrall, M. Kubicki, and M. Sikorski, New photochemically stable riboflavin analogue—3-methyl-riboflavin tetraacetate, J. Photochem. Photobiol. A **186**, 14 (2007).

[20] D. E. Metzler and W. L. Cairns, Photochemical degradation of flavines. VI. New photoproduct and its use in studying the photolytic mechanism, J. Am. Chem. Soc. **93**, 2772 (1971).

[21] I. Ahmad and H. D. C. Rapson, Multicomponent spectrophotometric assay of riboflavine and photoproducts, J. Pharm. & Biomed. Anal. **8**, 217.

[22] M. Insińska-Rak, D. Prukała, A. Golczak, E. Fornal, and M. Sikorski, Riboflavin degradation products; combined photochemical and mass spectrometry approach, J. Photochem. Photobiol. A **403**, 112837 (2020).

[23] M. A. Sheraz, S. H. Kazi, S. Ahmed, Z. Anwar, and I. Ahmad, Photo, thermal and chemical degradation of riboflavin, Beilstein J. Org. Chem. (2014).

[24] W. M. Moore and C. Baylor Jr., Photochemistry of riboflavine. IV. Photobleaching of some nitrogen-9 substituted isoalloxazines and flavines, J. Am. Chem. Soc. **91**, 7170 (1969).

[25] W. Holzer, A. Penzkofer, T. Susdorf, M. Álvarez, Sh. D. M. Islam, and P. Hegemann, Absorption and emission spectroscopic characterisation of the LOV2-domain of phot from Chlamydomonas reinhardtii fused to a maltose binding protein, Chem. Phys. **302**, 105 (2004).

[26] W. Holzer, A. Penzkofer, and P. Hegemann, Absorption and emission spectroscopic characterisation of the LOV2-His domain of phot from Chlamydomonas reinhardtii, Chem. Phys. **308**, 79 (2004).

[27] G. K. Radda and M. Calvin, Chemical and photochemical reductions of flavin nucleotides and analogs, Biochemistry **3**, 384–393 (1964).

[28] B. Holmström, A metastable intermediate in the anaerobic photolysis of riboflavin, Bull. Soc. Chim. Belges **71**, 869 (1962).

[29] P.-S. Song and D. E. Metzler, Photochemical degradation of flavins. IV. Studies of the anaerobic photolysis of riboflavin, Photochem. & Photobiol. **6**, 691 (1967).

[30] I. Ahmad, Q. Fasihullah, A. Noor, I. A. Ansari, and Q. N. M. Ali, Photolysis of riboflavin in aqueous solution: a kinetic study, Int. J. Pharm. **280**, 199 (2004).

[31] S. Salzmann, J. Tatchen, and C. M. Marian, The photophysics of flavins: What makes the

difference between gas phase and aqueous solution?, J. Photochem. Photobiol. A **198**, 221 (2008).

[32] M.P. Kabir, Y. Orozco-Gonzalez, and S. Gozem, Electronic spectra of flavin in different redox and protonation states: a computational perspective on the effect of the electrostatic environment, Phys. Chem. Chem. Phys. **21**, 16526 (2019).

[33] M.P. Kabir, D. Ouedraogo, Y. Orozco-Gonzalez, G. Gadda, and S. Gozem, Alternative strategy for spectral tuning of flavin-binding fluorescent proteins, J. Phys. Chem. B **127**, 1301 (2023).

[34] K. Zenichowski, M. Gothe, and P. Saalfrank, Exciting flavins: Absorption spectra and spin–orbit coupling in light–oxygen–voltage (LOV) domains, J. Photochem. Photobiol. A **190**, 290.

[35] S. Salzmann, M. R. Silva-Junior, W. Thiel, and C. M. Marian, Influence of the lov domain on low-lying excited states of flavin: A combined quantum-mechanics/molecular-mechanics investigation, J. Phys. Chem. B **113**, 15610 (2009).

[36] B. F. Minaev, H. Ågren, and V. O. Minaeva, *Handbook of Computational Chemistry*, chapter Spin–Orbit Coupling in Enzymatic Reactions and the Role of Spin in Biochemistry, pages 1–31. Springer, 2016.

[37] M. Bracker, M. K. Kubitz, C. Czekelius, C. M. Marian, and M. Kleinschmidt, Computer-aided design of fluorinated flavin derivatives by modulation of intersystem crossing and fluorescence, ChemPhotoChem **6**, e202200040 (2022).

[38] P. R. Ogilby, Singlet oxygen: there is indeed something new under the sun, Chem. Soc. Rev. **39**, 3181 (2010).

[39] T. Föerster, Zwischenmolekulare energiewanderung und fluoreszenz, Ann. Phys. **2**, 55 (1948).

[40] D. L. Dexter, A theory of sensitized luminescence in solids, J. Chem. Phys. **21**, 836 (1953).

[41] H. Kautsky, Quenching of luminescence by oxygen, Trans. Faraday Soc. **35**, 216 (1938).

[42] H. Tsubomura and R. S. Mulliken, Molecular complexes and their spectra. XII. Ultraviolet absorption spectra caused by the interaction of oxygen with organic molecules, J. Am. Chem. Soc. **82**, 5966 (1960).

[43] K. Kawaoka, A. U. Khan, and D. R. Kearns, Role of singlet excited states of molecular oxygen in the quenching of organic triplet states, J. Chem. Phys. **46**, 1842 (1967).

[44] B. F. Minaev, Quantum-chemical investigation of the mechanisms of the photosensitization, luminescence, and quenching of singlet $^1\Delta_g$ oxygen in solutions, Zhurnal Prikladnoi Spektroskopii **42**, 766 (1985), https://link.springer.com/article/10.1007/BF00661398.

[45] B. F. Minaev, V. V. Bryukhanov, G. A. Ketsle, V. Ch. Laurinas, Z. M. Muldakhmetov, Zh. K. Smagulov, , and K. F. Regir, Interaction mechanism of molecular oxygen with excited states of luminophores in solution, in polymers, and at a surface, Zhurnal Prikladnoi Spektroskopii **50**, 291 (1989), https://link.springer.com/article/10.1007/BF00659989.

[46] M.B. Smith and J. Michl, Recent advances in singlet fission, Annu. Rev. Phys. Chem. **64**, 361 (2013).

[47] D. Casanova, Theoretical modeling of singlet fission, Chem. Rev. **118**, 7164 (2018).

[48] A. Warshel and M. Levitt, Theoretical studies of enzymatic reactions: Dielectric electrostatic and steric stabilization of the carbonium ion in the reaction of lysozyme, J. Mol. Biol. **103**, 227 (1976).

[49] H. M. Senn and W. Thiel, QM/MM methods for biomolecular systems, Angew. Chem., Int. Ed. **48**, 1198 (2009).

[50] I. Polyakov, A. Kulakova, and A.V. Nemukhin, Computational modeling of the interaction of molecular oxygen with the miniSOG protein—a light induced source of singlet oxygen, Biophysica **3**, 252 (2023).

[51] R. B. Best, X. Zhu, J. Shim, P. E. M. Lopes, J. Mittal, M. Feig, and A. D. MacKerell, Optimization of the additive charmm all-atom protein force field targeting improved sampling of the backbone ϕ, ψ and side-chain χ_1 and χ_2 dihedral angles, J. Chem. Theory Comput. **8**, 3257 (2012).

[52] A. Alexandrov, Molecular mechanics model for flavins, J. Comput. Chem. **40**, 2834 (2019).

[53] J.P. Perdew, K. Burke, and M. Ernzerhof, Generalized gradient approximation made simple, Phys. Rev. Lett. **77**, 3865 (1996).

[54] J. W. Ponder and D. A. Case, Force fields for protein simulations, Adv. Prot. Chem. **66**, 27 (2003).

[55] D. Casanova and M. Head-Gordon, Restricted active space spin-flip configuration interaction approach: Theory, implementation and examples, Phys. Chem. Chem. Phys. **11**, 9779 (2009).

[56] A.A. Granovsky, Extended multi-configuration quasi-degenerate perturbation theory: The new approach to multi-state multi-reference perturbation theory, J. Chem. Phys. **134**, 214113 (2011).

[57] G. Herzberg, *Molecular spectra and molecular structure: I. Spectra of diatomic molecules*, volume I. van Nostrand Reinhold: New York, 1950.

[58] A. I. Krylov, The quantum chemistry of open-shell species, in *Reviews in Comp. Chem.*, edited

by A. L. Parrill and K. B. Lipkowitz, volume 30, pages 151–224. J. Wiley & Sons, 2017.

[59] A. I. Krylov, Size-consistent wave functions for bond-breaking: The equation-of-motion spin-flip model, Chem. Phys. Lett. **338**, 375 (2001).

[60] D. Casanova and A. I. Krylov, Spin-flip methods in quantum chemistry, Phys. Chem. Chem. Phys. **22**, 4326 (2020).

[61] X. Feng, A. V. Luzanov, and A. I. Krylov, Fission of entangled spins: An electronic structure perspective, J. Phys. Chem. Lett. **4**, 3845 (2013).

[62] X. Feng and A. I. Krylov, On couplings and excimers: Lessons from studies of singlet fission in covalently linked tetracene dimers, Phys. Chem. Chem. Phys. **18**, 7751 (2016).

[63] X. Feng, D. Casanova, and A. I. Krylov, Intra- and inter-molecular singlet fission in covalently linked dimers, J. Phys. Chem. C **120**, 19070 (2016).

[64] B. A. Hess, C. M. Marian, U. Wahlgren, and O. Gropen, A mean-field spin-orbit method applicable to correlated wavefunctions, Chem. Phys. Lett. **251**, 365 (1996).

[65] C. M. Marian, Spin-orbit coupling and intersystem crossing in molecules, WIREs: Comput. Mol. Sci. **2**, 187 (2012).

[66] P. Pokhilko, E. Epifanovsky, and A. I. Krylov, General framework for calculating spin–orbit couplings using spinless one-particle density matrices: theory and application to the equation-of-motion coupled-cluster wave functions, J. Chem. Phys. **151**, 034106 (2019).

[67] A. Carreras, H. Jiang, P. Pokhilko, A. I. Krylov, P. M. Zimmerman, and D. Casanova, Calculation of spin-orbit couplings using RASCI spinless one-particle density matrices: Theory and applications, J. Chem. Phys. **153**, 214107 (2020).

[68] A. I. Krylov and P. M. W. Gill, Q-Chem: An engine for innovation, WIREs: Comput. Mol. Sci. **3**, 317 (2013).

[69] E. Epifanovsky, A. T. B. Gilbert, X. Feng, J. Lee, Y. Mao, N. Mardirossian, P. Pokhilko, A. F. White, M. P. Coons, A. L. Dempwolff, Z. Gan, D. Hait, P. R. Horn, L. D. Jacobson, I. Kaliman, J. Kussmann, A. W. Lange, K. U. Lao, D. S. Levine, J. Liu, S. C. McKenzie, A. F. Morrison, K. D. Nanda, F. Plasser, D. R. Rehn, M. L. Vidal, Z.-Q. You, Y. Zhu, B. Alam, B. J. Albrecht, A. Aldossary, E. Alguire, J. H. Andersen, V. Athavale, D. Barton, K. Begam, A. Behn, N. Bellonzi, Y. A. Bernard, E. J. Berquist, H. G. A. Burton, A. Carreras, K. Carter-Fenk, R. Chakraborty, A. D. Chien, K. D. Closser, V. Cofer-Shabica, S. Dasgupta, M. de Wergifosse, J. Deng, M. Diedenhofen, H. Do, S. Ehlert, P.-T. Fang, S. Fatehi, Q. Feng, T. Friedhoff,

J. Gayvert, Q. Ge, G. Gidofalvi, M. Goldey, J. Gomes, C. E. González-Espinoza, S. Gulania, A. O. Gunina, M. W. D. Hanson-Heine, P. H. P. Harbach, A. Hauser, M. F. Herbst, M. Hernández Vera, M. Hodecker, Z. C. Holden, S. Houck, X. Huang, K. Hui, B. C. Huynh, M. Ivanov, Á. Jász, H. Ji, H. Jiang, B. Kaduk, S. Kähler, K. Khistyaev, J. Kim, G. Kis, P. Klunzinger, Z. Koczor-Benda, J. H. Koh, D. Kosenkov, L. Koulias, T. Kowalczyk, C. M. Krauter, K. Kue, A. Kunitsa, T. Kus, I. Ladjánszki, A. Landau, K. V. Lawler, D. Lefrancois, S. Lehtola, R. R. Li, Y.-P. Li, J. Liang, M. Liebenthal, H.-H. Lin, Y.-S. Lin, F. Liu, K.-Y. Liu, M. Loipersberger, A. Luenser, A. Manjanath, P. Manohar, E. Mansoor, S. F. Manzer, S.-P. Mao, A. V. Marenich, T. Markovich, S. Mason, S. A. Maurer, P. F. McLaughlin, M. F. S. J. Menger, J.-M. Mewes, S. A. Mewes, P. Morgante, J. W. Mullinax, K. J. Oosterbaan, G. Paran, A. C. Paul, S. K. Paul, F. Pavošević, Z. Pei, S. Prager, E. I. Proynov, Á. Rák, E. Ramos-Cordoba, B. Rana, A. E. Rask, A. Rettig, R. M. Richard, F. Rob, E. Rossomme, T. Scheele, M. Scheurer, M. Schneider, N. Sergueev, S. M. Sharada, W. Skomorowski, D. W. Small, C. J. Stein, Y.-C. Su, E. J. Sundstrom, Z. Tao, J. Thirman, G. J. Tornai, T. Tsuchimochi, N. M. Tubman, S. P. Veccham, O. Vydrov, J. Wenzel, J. Witte, A. Yamada, K. Yao, S. Yeganeh, S. R. Yost, A. Zech, I. Y. Zhang, X. Zhang, Y. Zhang, D. Zuev, A. Aspuru-Guzik, A. T. Bell, N. A. Besley, K. B. Bravaya, B. R. Brooks, D. Casanova, J.-D. Chai, S. Coriani, C. J. Cramer, G. Cserey, A. E. DePrince, R. A. DiStasio, A. Dreuw, B. D. Dunietz, T. R. Furlani, W. A. Goddard, S. Hammes-Schiffer, T. Head-Gordon, W. J. Hehre, C.-P. Hsu, T.-C. Jagau, Y. Jung, A. Klamt, J. Kong, D. S. Lambrecht, W. Liang, N. J. Mayhall, C. W. McCurdy, J. B. Neaton, C. Ochsenfeld, J. A. Parkhill, R. Peverati, V. A. Rassolov, Y. Shao, L. V. Slipchenko, T. Stauch, R. P. Steele, J. E. Subotnik, A. J. W. Thom, A. Tkatchenko, D. G. Truhlar, T. Van Voorhis, T. A. Wesolowski, K. B. Whaley, H. L. Woodcock, P. M. Zimmerman, S. Faraji, P. M. W. Gill, M. Head-Gordon, J. M. Herbert, and A. I. Krylov, Software for the frontiers of quantum chemistry: An overview of developments in the Q-Chem 5 package, J. Chem. Phys. **155**, 084801 (2021).

[70] A. A. Granovsky, XMCQDPT2, URL http://classic.chem.msu.su (Accessed Dec. 18, 2009).

[71] M. A. El-Sayed, Triplet state: Its radiative and non-radiative properties, Acc. Chem. Res. **1**, 8 (1968).

[72] M. Alessio, S. Kotaru, G. Giudetti, and A. I. Krylov, Origin of magnetic anisotropy in nickelocene molecular magnet and resilience of its magnetic behavior, J. Phys. Chem. C **127**, 3647 (2023).

[73] M. Weldon, T. D. Poulsen, K. V. Mikkelsen, and P. R. Ogilby, Singlet sigma: The "other" singlet oxygen in solution, Photochem. and Photobiol. **70**, 369 (1999).

[74] T. J. Penfold, E. Gindensperger, C. Daniel, and C. M. Marian, Spin-vibronic mechanism for intersystem crossing, Chem. Rev. **118**, 6975 (2018).

[75] C. Marian, Understanding and controlling intersystem crossing in molecules, Annu. Rev. Phys. Chem. **72**, 617 (2021).

[76] D. Casanova, L. V. Slipchenko, A. I. Krylov, and M. Head-Gordon, Double spin-flip approach within equation-of-motion coupled cluster and configuration interaction formalisms: Theory, implementation and examples, J. Chem. Phys. **130**, 044103 (2009).

[77] S. Matsika, X. Feng, A. V. Luzanov, and A. I. Krylov, What we can learn from the norms of one-particle density matrices, and what we can't: Some results for interstate properties in model singlet fission systems, J. Phys. Chem. A **118**, 11943 (2014).

[78] M. Kasha, Characterization of electronic transitions in complex molecules, Disc. Faraday Soc. **9**, 14 (1950).

[79] B. F. Minaev, Theoretical model of triplet–triplet annihilation, Izvestiya Vysshikh Uchebnykh Zavedenii, Fizika , 12 (1977), English version: Plenum Publishing Corporation, 0038-5697/78/2109-1120, 1979.

[80] M.J.Y. Tayebjee, D.R. McCamey, and T.W. Schmidt, Beyond Shockley-Queisser: Molecular approaches to high-efficiency photovoltaics, J. Phys. Chem. Lett. **6**, 2367 (2015).

[81] D. L. Dexter, Two ideas on energy transfer phenomena: Ion-pair effects involving the OH stretching mode, and sensitization of photovoltaic cells, J. Lumin. **18-19**, 779 (1979).